3. S. A. Bostandzhiyan, V. I. Boyarchenko, et al., "Low-temperature modes of polymerization in a flow reactor," Zh. Prikl. Mekh. Tekh. Fiz., No. 1 (1979).
4. L. G. Laitsyanskii, Mechanics of Liquids and Gases [in Russian], Nauka, Moscow (1970).
5. D. A. Vaganov, "Some two-dimensional effects in the flow of a reacting liquid whose properties vary with extent of reaction," Zh. Prikl. Mekh. Tekh. Fiz., No. 1 (1977).
6. D. A. Vaganov, "Quasistationary flow of a reacting liquid that loses fluidity at high degrees of reaction," Zh. Prikl. Mekh. Tekh. Fiz., No. 3 (1982).

FORCE CHARACTERISTICS AND FLOW PARAMETERS IN COMBUSTION MODELS

V. K. Baev, V. V. Shumskii, and M. I. Yaroslavtsev

UDC 536.46:621.45.022

In [1] we find results on the force characteristics and flow parameters in the internal section of a gasdynamic model with combustion in a pulsed wind tunnel at a Mach number in the incident flow $M_i = 7.3$, the combustion being determined because the energy aspects of the IT-301 pulsed tunnel [2] allow one to have a four-chamber volume of not more than about 1.2 dm^3 subject to the condition of providing pressures and temperatures sufficient for self-ignition of the hydrogen in the model. This four-chamber volume provides a diameter for the critical nozzle section of not more than about 10 mm on the basis of the maximum possible rate of fall in the incident air flow parameters allowing the forces and pressures to be measured, which with the model dimensions of [1] $d_0 = 72$ mm gave the minimum possible value at $M_i = 7$-7.5, where d_0 is the diameter of the inlet to the air intake in the model.

The positive results of [1] as regards the internal working process and force characteristics lead one to ask whether one can reduce M_i by reducing the dimensions of the model with the same tunnel energy and with the same rates of fall in the parameters? Therefore, a model with $d_0 = 23$ mm was devised, which enabled one to reduce the Mach number of the incident air flow to $M_i = 4.9$. The present paper is based on the results obtained with this model in a high-enthalpy air flow.

The model (Fig. 1) is a combination of the air intake and a chamber placed between Secs. 2 and 5, in which the hydrogen supplied to the model burns. The inner part of the model either had the critical section at the exit (form 1) or did not have a critical section (form 2); then the expansion factors in the combustion chamber $\overline{F}_c = F_5/F_2$ were 2.92 and 3.75 for forms 1 and 2 correspondingly, where F_5 and F_2 are the areas of cross section at the exit from the combustion chamber in Sec. 5 and at the inlet in Sec. 2.

The model was set up in the working part of the pulsed tunnel along the axis of the profiled nozzle on the lateral pillar 1 covered by the aerofoil 2. The pillar was attached to a mechanical device serving to isolate the longitudinal component from the total aerodynamic force. This device in turn was connected to a one-component aerodynamic balance [3]. The model contained no volume where the hydrogen could be stored, in contrast to the model of [1], so the hydrogen was supplied from an external cylinder of capacity 120-150 cm^3 through the supporting pillar.

The hydrogen was injected through two supply rings 3 and 4 through holes of diameter 1 mm drilled at 45° in the opposite direction to the flow: In the front ring 3 there were eight holes, and in the rear ring 4 there were six. About 60% of the hydrogen was supplied through the front ring and about 40% through the rear one.

The experiments were performed with the following ranges in the incident air parameters: stagnation pressure and temperature $p_{0i}(\tau) = 60$-70 MPa, $T_{0i}(\tau) = 1850$-1000°K, static temperature and pressure $p_i(\tau) = 1100$-150 hPa, $T_i(\tau) = 350$-180°K, dynamic head $q_i(\tau) = 1.8$-0.25 MPa, $M_i = 4.9$, air flow rate through model 0.85-0.14 kg/sec, and Reynolds number $Re(\tau) = v_i(\tau)/\nu_i(\tau) = (100\text{-}30)\cdot 10^6$ 1/m, where v_i and ν_i are the velocity and kinematic viscosity of the incident air. Here $\tau = 0$-50 msec is the current time, the origin being reckoned from the instant of discharging a capacitor bank in the forechamber. The rates of fall in the parameters

Novosibirsk. Translated from Zhurnal Prikladnoi Mekhaniki i Tekhnicheskoi Fiziki, No. 1, pp. 103-109, January-February, 1984. Original article submitted December 22, 1982.

0021-8944/84/2501-0093$08.50

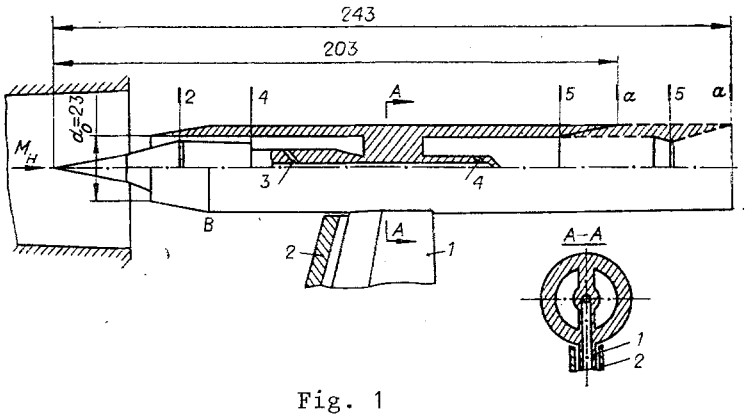

Fig. 1

were close to those of [4] under the conditions typical of these pulsed tubes with the forechamber of volume 1.14 dm^3, diameter of the critical nozzle section 10 mm, and charging voltage for the capacitor bank U = 4-4.2 kV.

The model did not fit completely into the Mach rhomb, and therefore it was set up at a distance from the end of the nozzle such that point B (Fig. 1) was in the Mach rhomb. Then the perturbations in the working part of the tube lay on the cylindrical part of the model and did not participate in producing the longitudinal force.

The experiments were performed with various relative areas for the throat of the intake $f_2 = F_2/F_0$, where $F_0 = \pi d_0^2/4$, and these showed that it was possible for the model to operate without breakaway in the aid flow throughout the operation of the pulsed tube only for $f_2 > 0.26$. For smaller values of f_2, the intake broke away, and the earlier the smaller f_2. The reason for this is associated with increased boundary-layer detachment on the central body at the point of incidence of the shock wave reflected from the housing [5].

To determine the expected parameter range, we calculated the force characteristics and parameters for form 2 under the test conditions. We varied $\bar{F}_c$, T_i, M_i, the excess-air coefficient α, and the combustion completeness ξ. The parameters were calculated for characteristic sections with allowance for the mass input and the actual properties of the combustion products for conditions of chemical and energy equilibrium [6, 7]. The calculations indicated as follows.

1. For $M_i = 4.9$ and $T_i < 350°K$, as used in the experiments, the heat input from the combustion of hydrogen with $\alpha = 0.5$-1 and $\xi > 0.5$ related to a subsonic gas flow in the combustion chamber.
2. There is a marked effect on the force characteristics from the internal section of the model from the extent of expansion $\bar{F}_c$ in the combustion chamber. For example, with $M_i = 4.9$, an increase in $\bar{F}_c$ from the minimum possible 1.59 (for $M_i = 4$) to 3.75 led to the specific force characteristics deteriorating by about 40%.
3. The pressure level in the combustion chamber falls as $\bar{F}_c$ increases, and at the same time there is an increase in the degree of incomplete expansion of the working body at the exit.
4. The internal-thrust coefficient $C_R = R/(q_i F_0)$ as a function of T_i is determined by the change in the relative heating with T_i, where R is the internal thrust, i.e., the force applied only to the internal surfaces in the model.

Figure 2 shows the variation in thrust coefficient $C_{F_M} = \bar{F}_M/(q_i F_0)$ with working time, where F_m is the model thrust measured by the balance. For form 1 (curve 1), the excess-air coefficient varied from $\alpha = 0.55$ at the start in this mode to $\alpha = 0.65$ at the end, while in form 2 (curve 2) the range was from $\alpha = 0.7$ at the start to $\alpha = 0.5$ at the end.

Figure 2 shows that in the region of $\tau \approx 20$ msec there is a kink in the $C_{F_M} = f(\tau)$ curve, which is due to reconstruction of the flow in the combustion chamber, which goes from supersonic during the first few milliseconds to subsonic, and this was the same as in the model of [1] in tests at $M_i = 7.3$. The time required for this is about 20 msec. In form 2, this time was somewhat greater than for form 1, which was due to the greater expansion of the combustion chamber in form 2 and therefore the need for greater relative heating to change the

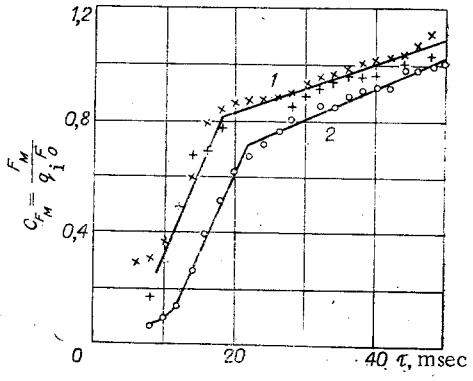

Fig. 2

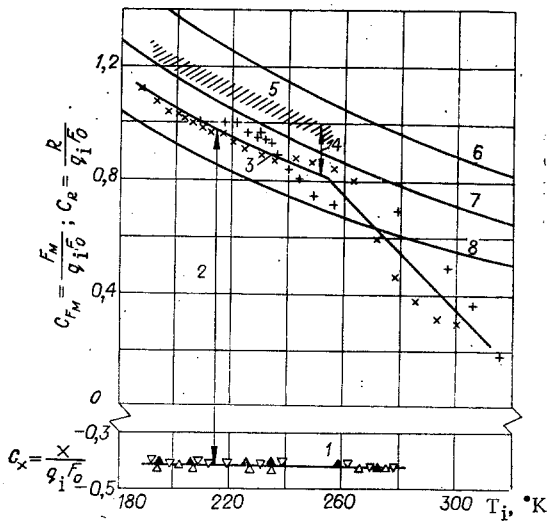

Fig. 3

heat-supply mode in form 2 relative to form 1. It has been shown [1] that after the end of the transient response in the combustion chamber, the hydrogen burns on average in a subsonic flow. The thrust in form 2 was less than that in form 1, as followed from the calculations on the effects of F_c on the internal thrust characteristics.

Figure 3 gives the thrust and resistance in relation to T_i, and it compares the experimental and calculated values for the internal-thrust coefficient.

One can compare the resistance coefficient $C_X = X/q_iF_0$ for this model (curve 1), where X is the resistance measured by the balance, with the resistance coefficient for the model of [1] with $M_i = 7.3$; the C_X are similar and fall in the range $C_X = 0.41$-0.44. Figure 3 shows that when subsonic combustion is established, the values of C_{F_M} for the various T_i may be approximated by the single curve 3 characterizing the thrust, i.e., a force applied to all surfaces both internal and external. The difference 2 between the model thrust and the resistance in the absence of hydrogen supply characterizes the effect from burning the hydrogen.

One usually operates with the internal thrust in calculations on thrust characteristics. This thrust R is greater than the F_m measured by the balance by the resistance of the housing and also by the amount of thrust produced by the working body because of the heat lost in the walls of the model. Region 5 in Fig. 3 was derived by adding the housing resistance to the model thrust, this being determined from a two-dimensional calculation of the flow over the outer surfaces and the heat losses derived from data on heat transfer to a flat plate [8] (segment 4 in Fig. 3), and this gives the experimental values for the internal-thrust coefficient G_R. Region 5 can be compared with the calculated values of C_R, and those given in Fig. 3 were derived with the following parameters: $\alpha = 0.6$, model nozzle velocity coefficient $\varphi_n = 0.98$, and combustion factor $\xi = 1$, 0.9, and 0.8 (curves 6-8 correspondingly).

The calculated and experimental values show as follows.

1. The experimental C_R increase as T_i decreases, and they coincide with the theoretical $C_R = f(T_i)$ relationship, i.e., the decisive factor for C_R in the experiments was the relative heating of the working body.
2. The completeness of combustion for the hydrogen corresponding to the observed C_R was in the range 0.9-0.95 for $T_i = 260$-$190°K$.
3. As T_i falls, the extent of combustion falls slightly, because p_i also falls as T_i decreases (as the mode time τ increases): p_i falls by about a factor 10 during $\tau = 50$ msec, and T_i by a factor 1.8-2, i.e., as the time increases, the hydrogen combustion conditions deteriorate, so there is less complete combustion at lower T_i.

The higher values of the combustion in our model ($\xi = 0.9$-0.95) relative to the model of [1] ($\xi = 0.7$-0.9) are due to the following factors: the better distribution of the hydrogen over the cross section of the combustion chamber, since in the model of [1] each hole served part of the chamber (ring) with cross-sectional dimensions of $\sim$12.5 × 8.5 mm, whereas in our model it served part of the ring with dimensions 7.1 × 4.7 mm, and the hydrogen was

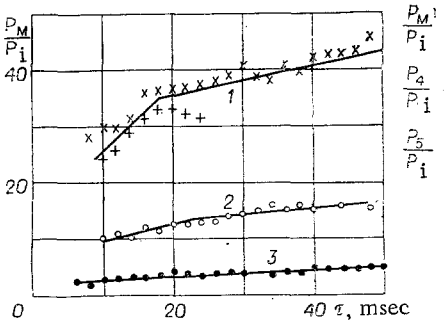

Fig. 4

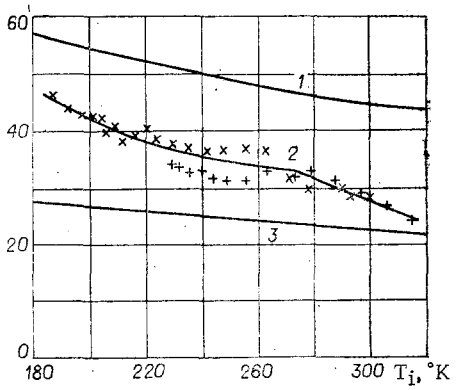

Fig. 5

supplied in an echelon fashion in our model, whereas it was supplied in a single section in [1], and finally the pressure in the combustion chamber in our model was higher by a factor 5-7 than that in the model of [1], while it should be noted that the level of $T_{0i}(\tau)$ in our experiments was approximately the same as that in the model of [1].

In all the experiments we measured the pressure p_M in the combustion chamber, with the static-pressure detector hole in the central part of the model in the housing behind the pillar. Figure 4 gives the observed pressures in the combustion chamber in relation to time, where 1 relates to form 1, α = 0.55-0.65, and 2 to form 2, α = 0.7-0.5, while 3 is for no hydrogen supply. As the expansion of the combustion chamber in form 1 is less than that in form 2, the degree of compression in the internal section is greater in form 1 than in form 2, so the pressure in form 1 on igniting the hydrogen is higher than that in form 2, which agrees completely with the above conclusions from the calculations.

The force characteristics indicate that the duration of the transient response in the model was about 20 msec. Figure 4 also implies a transient in the combustion chamber. The duration of this as determined from the pressure in the combustion chamber agrees very closely with that derived from the thrust measurements.

There is a considerable increase in the pressure in the combustion chamber in form 1 on supplying hydrogen with $\alpha \approx 0.6$; the pressure when the hydrogen burns is raised by a factor 9-11 by comparison with that in the absence of hydrogen, which is higher than in the model of [1], where the corresponding increase was by a factor 4-5. This occurs although the chamber expansion in our model is much greater than that in [1]: 2.92 by comparison with 1.884 in [1]. The reason for the larger pressure increase is that the relative hydrogen flow rate in our model was larger by almost a factor three: The experiments with the model were based on $\alpha \approx 0.6$, while those with the model of [1] were with $\alpha \approx 1.7$.

Figure 5 compares the measured p_M for form 1 with the calculated exit pressure curves (in Sec. 5) and those for Sec. 4, namely the section of the combustion chamber where heat begins to be supplied to it in the calculation scheme [1, 6] (1 and 3 are from calculation and 2 is from experiment, with 1 representing p_4/p_i, 2 representing p_M/p_i, and 3 representing p_5/p_i, where p_4 and p_5 are the pressures in Secs. 4 and 5 correspondingly). The calculation was performed with the parameters used with form 1: α = 0.6, ξ = 0.9. Figure 5 shows that p_M as measured agrees closely with the calculated value: p_M should fall between the pressure in Sec. 4 (curve 1) and that in Sec. 5 (curve 3), as occurs.

The theoretical curves 1 and 3 were obtained with heat supplied to the chamber in subsonic flow. Figure 5 also confirms the fact established from the force measurements and the calculations: The heat supplied in the chamber after the end of the transient occurs in this model on average with a subsonic flow in the combustion chamber. If the situation were otherwise, p_M would lie far below curve 3, since the maximum pressure in the combustion chamber occurs at Sec. 5 on supplying heat to a supersonic flow; the pressures in all other sections of the combustion chamber are less than that in Sec. 5 when heat is supplied to a supersonic flow in it.

The tests on the model of Fig. 1 were accompanied by tests at M_i = 4.9 and the same incident air flow parameters for a model in which the air intake was one with completely internal compression (Fig. 6). The main data on the working process and force characteristics during combustion were obtained in the experiments with the model of [1] at M_i = 7.3 and in

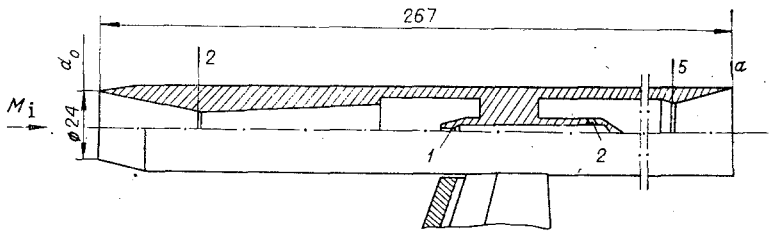

Fig. 6

the experiments with M_i = 4.9 with the model shown in Fig. 1. The model shown in Fig. 6 on the other hand was used in a restricted number of experiments designed mainly to confirm the results obtained with the previous two models. The model of Fig. 6 is a combination of an air intake with complete internal compression, a combustion chamber (part between Secs. 2-5), and a nozzle (part 5-a). The central part, the pillar, the pillar air foil, and the nozzle part were assembled from the same items for the models shown in Figs. 1 and 6. Hydrogen was supplied to the model through two rings: the leading ring 1 and the rear ring 2. Jets of various types were used in the leading ring in the different experiments: single jets of diameter from 1 to 4 mm, and jets each consisting of a set of 6-8 holes of diameter 1 mm drilled at 45° either against the flow or along it. The model with the internal-compression intake was tested with burning hydrogen at f_2 = 0.24, although f_2 = 0.16 also provided normal air flow throughout the tube operation. The following results were obtained with the model of Fig. 6 with α = 1.7-0.8.

1. The flow is rearranged over 20-26 msec in the internal section of the model because of the change in heat-supply conditions from supersonic to sonic.
2. The falls in p_i, T_i, and α during the work mode led to flow breakaway at α = 0.8-0.9. The value of C_{FM} directly before breakaway was 1-1.2. As in the previous models, the breakaway was related to the effects of the combustion chamber on the intake: altering the method of supplying the hydrogen to the front ring and the geometry of the initial part of the chamber enabled us to avoid breakaway throughout the operation.
3. The thrust characteristics corresponded with the calculated values, and their variation with time (with T_i) was determined by the time course of the relative working-body heating.

Therefore, these results with an internal-compression intake confirm those obtained with the model of [1] and with that of Fig. 1.

Therefore, the following results are obtained from the calculations and experiments with three gas-dynamic models using combustion (one model with d_0 = 72 mm for M_i = 7.3 [1] and two models with d_0 = 23-24 mm with M_i = 4.9):

1) In all the models, the flow in the section of the model and the dependence on T_i were the same (the flow mode is determined by the relative heating of the working body);
2) hydrogen supply against the flow with a small recirculation zone provides high completeness in the combustion with a length of only 130-180 mm for the combustion chamber with a subsonic air flow (up to ξ = 0.9-0.95) and without any adverse effect from the combustion chamber on the intake;
3) the force characteristics found by experiment correspond to the calculated ones, i.e., the calculation method is in agreement with the experimental data.

LITERATURE CITED

1. V. K. Baev, V. V. Shumskii, and M. I. Yaroslavtsev, "A study of the operation of the two-mode combustion chamber with subsonic heat supply," in: Gasdynamic Flows in Nozzles and Diffusers [in Russian], Novosibirsk (1982); "Research on the gasdynamics of a model with combustion in a pulsed wind tunnel," Zh. Prikl. Mekh. Tekh. Fiz., No. 6 (1983).
2. A. S. Korolev, B. V. Boshenyatov, I. G. Druker, and V. V. Zatoloka, Pulsed Wing Tunnels in Aerodynamic Research [in Russian], Nauka, Novosibirsk (1978).
3. S. V. Belousov, V. V. Golod, Yu. A. Pronin, and M. I. Yaroslavtsev, "Balance tests on heavy models in pulsed mode at hypersonic velocities," in: Methods and Techniques in Aerodynamic Research [in Russian], ITPM Sib. Otd. Akad. Nauk SSSR, Novosibirsk (1978).

4. V. K. Baev, B. V. Boshenyatov, Yu. A. Pronin, and V. V. Shumskii, "An experimental study of the ignition of hydrogen injected into a supersonic flow of hot air," in: Gasdynamics of Combustion in a Supersonic Flow [in Russian], ITPM Sib. Otd. Akad. Nauk SSSR, Novosibirsk (1979).
5. V. G. Gurylev and E. V. Piotrovich, "Flow breakaway at the inlet of a supersonic air intake," Uchen. Zap. TsAGI, 5, No. 3 (1974).
6. Yu. A. Saren and V. V. Shumskii, "Characteristics of a hypersonic jet engine with a two-mode combustion chamber," in: Gasdynamics of Flows in Nozzles and Diffusers [in Russian], ITPM Sib. Otd. Akad. Nauk SSSR, Novosibirsk (1982).
7. V. E. Alemasov, A. F. Dregalin, A. P. Tishin, and V. A. Khudyakov, Thermodynamic and Thermophysical Properties of Combustion Products [in Russian], Vol. 1, Nauka, Moscow (1971).
8. V. M. Kovalenko, "Calculations of turbulent-flow and heat-transfer coefficients for a smooth plate at supersonic velocities in the presence of heat transfer," Trudy TsAGI, Issue 1084 (1967).

SELF-MODELING PARAMETER DISTRIBUTION BEHIND A DETONATION WAVE

V. N. Okhitin

UDC 534.222.2

An analytic solution exists only in the planar case to the self-modeling problem of the parameter distribution behind a stationary detonation-wave front in a perfect gas [1]. Numerical solutions have been derived for waves of spherical and cylindrical symmetries by the use of various equations of state for detonation products DP [2-4]. There are also analytic approximations for the distributions behind the fronts of symmetrical detonation waves DW in condensed explosives [4, 5], which are interesting for use as initial conditions in solving more complex detonation problems. Numerical calculations show that the behavior of the DP from gaseous explosives [6] and condensed ones of various densities [4, 5] can be described quite accurately from the isentropic relation between the pressure p and density ρ for a perfect gas with various values of the adiabatic parameter γ. It is therefore of interest to derive analytical relationships for the self-modeling parameter distribution behind a stationary DW front for various types of symmetry and for the equation of state for a perfect gas whose adiabatic parameter varies over a wide range. Tight specifications are laid down for the analytic relationships on account of their use in numerical calculations. In particular, they should satisfy the asymptotic solutions in the region of the DW front and at the boundary with the central region at rest, and they should also describe the numerical solutions with sufficiently high accuracy.

Here we derive analytic relations for the self-modeling parameter distribution behind a stationary DW front in the Chapman–Jouguet mode for various forms of symmetry satisfying these requirements.

A system of ordinary differential equations in the self-modeling variable $\zeta = r/t$ describes the parameter distribution behind a stationary DW front [7]:

$$\frac{du}{d\zeta}\left[\frac{(\zeta-u)^2}{c^2}-1\right]=\frac{\nu u}{\zeta},\quad (\zeta-u)\frac{du}{d\zeta}=\frac{c^2}{\rho}\frac{d\rho}{d\zeta},$$

where ρ, u, and c are the density, mass velocity, and speed of sound, r and t are independent variables for the distance from the point of detonation initiation and time, and ν is the symmetry parameter, which takes the values 0, 1, and 2 correspondingly for planar, cylindrical, and spherical DW.

We introduce the dimensionless linear coordinate r/R, where R is the coordinate of the DW front, and use the fact that $c \sim \rho^{(\gamma-1)/2}$ for a perfect gas, whereupon the system can be reduced to

Moscow. Translated from Zhurnal Prikladnoi Mekhaniki i Tekhnicheskoi Fiziki, No. 1, pp. 109-113, January-February, 1984. Original article submitted December 1, 1982.

 0021-8944/84/2501-0098$08.50